sciendo
Polish Journal of Medical Physics and Engineering
The Journal of Polish Society of Medical Physics
ISSN 1898-0309, doi: 10.2478/pjmpe-2022-0022
December 2022
Vol 28, Issue 4

Scientific Paper

Construction and pre-evaluation of an in-house cylindrical ionization chamber fabricated from locally available materials

Samuel Nii Adu TAGOE [1,2,ACDEF,*], Clement Dominic CHAPHUKA [3,BC], Francis HASFORD [4,EF]

[1]*Department of Radiography, School of Biomedical and Allied Health Sciences, College of Health Sciences, University of Ghana, Ghana*
[2]*Department of Radiation Oncology, National Centre for Radiotherapy and Nuclear Medicine, Korle-Bu Teaching Hospital, Ghana*
[3]*Department of Health and Technology Support Service- Division of Physical Asset Management, Ministry of Health and Population, Malawi*
[4]*Radiological and Medical Sciences Research Institute, Ghana Atomic Energy Commission, Ghana*
[*]*Corresponding author: Samuel Nii Adu Tagoe; samniitagoe@yahoo.co.uk*

(received 26 June 2022; revised 23 August and 26 September 2022; accepted 23 October 2022)

Abstract

Introduction: The objectives of this study were to construct a very robust in-house cylindrical ionization chamber from locally available materials to minimize cost, and to assess its suitability for use in a clinical setting.

Materials and Methods: The entire body of the constructed IC was composed of Perspex (PMMA). Other components of the IC were made from locally available materials, such as paper and discarded items. The in-house IC was made waterproof by passing the triaxial cable connecting its various electrodes through a plastic tube which once served as a drainage tube of a urine bag. This connection was made such that the chamber was vented to the environment. The completed in-house IC was evaluated for: polarity effect, ion recombination, ion collection efficiency, stability, dose linearity, stem effect, leakage current, angular, dose rate and energy dependences.

Results: Although the pre-evaluation results confirmed that the in-house IC satisfied the stipulated international standards for ICs, there was a need to enhance the stem effect and leakage current characteristics of the IC. The in-house IC was found to have an absorbed dose to water calibration coefficient of 4.475 x 10^7 Gy/C (uncertainty of 1.6%) for cobalt 60 through a cross-calibration with a commercial 0.6 cc cylindrical IC with traceability to the Germany National Dosimetry Laboratory. Using a Jaffé diagram, the in-house IC was also found to have a recombination correction factor of 1.0078 when operated at the calibration voltage of + 400 V. In terms of beam quality correction factors for megavoltage beams, the in-house IC was found to exhibit characteristics similar to those of Scanditronix-Wellhofer IC 70 Farmer type IC.

Conclusion: The constructed in-house Farmer-type IC was able to meet all the recommended characteristics for an IC, and therefore, the in-house IC is suitable for beam output calibration in external beam radiotherapy.

Keywords: in-house ionization chamber; beam output calibration; Perspex; stem effect; leakage current.

Introduction

One of the dogmas of external beam radiotherapy (EBRT) is accurate dose delivery to the prescribed target volume. Regarding the International Commission on Radiological Unit (ICRU) recommendation of overall accuracy in tumour dose delivery of ±5%, based on analysis of dose-response data and evaluation of errors in dose delivery in a clinical setting[1,2]. Uncertainties associated with various processes leading to dose delivery to a patient should be marginal. One of the processes constituting the chain representing an accurate dose delivery to the patient is the determination of the output of the treatment machine being used to deliver the radiation dose to a patient.[3]

Determination of the output of a treatment machine is sometimes referred to as beam out calibration. Treatment machines are designed and configured such that the amount of radiation delivered to a patient is quantified in terms of treatment time or monitor unit. Concerning this, there is, therefore, the need to know accurately the output of a treatment machine for a set of reference irradiation geometry and conditions to facilitate the conversion of a prescribed dose at any point within a patient to treatment time or monitor unit. Recommendation with regards to this reference dosimetry is that the measurement should be done in water with an appropriate resolution dosimetry system using a field size of 10 cm × 10 cm and employing either source-to-surface distance (SSD) or isocentric irradiation technique.[4,5]

Authors' contribution:
A – Research concept and design, B – Collection and/or assembly of data, C – Data analysis and interpretation, D – Writing the article, E – Critical revision of the article, F – Final approval of the article.

It is very cumbersome trying to obtain treatment machine output for every irradiation geometry that will be used clinically. Dosimetric functions obtained via measurements in water for various irradiation geometries are used to find a link between the treatment machine output measured for the reference condition, and that is likely to be used in a clinical setting.[3] Dosimetry system, which is usually used for reference dosimetry, consists of a calibrated large volume (about 0.6 cm^3) cylindrical IC connected to a suitable electrometer, which is either calibrated separately or together.[6] The accuracy with which the beam output of a treatment machine is determined is influenced by the dosimetry system and the protocol adopted in the measurement of the treatment machine output.[3,5,7] The accuracy and precision of a dosimeter are very crucial and essential in reducing uncertainties associated with reference dosimetry. Most commercially available cylindrical ICs are designed to be precise but are quite expensive and very fragile. Precautionary measures are, therefore, needed in their handling to ensure that they are not damaged or their performances are not compromised.

Students or interns learning radiation metrology would require hands-on experience with these ICs and may be ignorant or adamant about precautionary measures needed to be observed in handling such dosimeters. Not adhering to the precautionary measures may cause severe damage to a dosimeter, culminating in cost implications. This study aims to design and construct a very rigid, robust and tough in-house cylindrical IC from locally available materials to minimise cost, and to ascertain the suitability of the constructed IC to be used by interns and medical physicists for teletherapy machine beam calibration and other radiation metrologies appropriate with the detector.

Materials

Materials that were used in the construction of the in-house cylindrical IC included:

i. A4 paper,
ii. 4B pencils,
iii. 20.0 cm length of solid Perspex (PMMA) rod with diameter of 15.9 mm,
iv. sterotape,
v. male thread Neil Concelman connector (TNC),
vi. low impedance triaxial cable,
vii. piece of twisted Aluminum cable,
viii. drainage tube of a urine bag, and
ix. multimeter.

The materials that were used to evaluate the performance of the constructed IC included:

i. PTW UNIDOS electrometer,
ii. PTW 0.6 cm^3 cylindrical IC,
iii. digital thermometer,
iv. aneroid barometer,
v. Equinox 100 Telecobalt machine,
vi. Elekta Synergy platform linear accelerator,
vii. IBA one-dimensional water phantom, and
viii. IBA Blue phantom[2].

Methods

The following processes and procedures were employed in the design and the construction of the in-house cylindrical IC as well as its pre-evaluation after construction. The pre-evaluation tests were carried out to ensure that the constructed cylindrical IC complies with the IEC 60731; 2011 recommendations for Farmer type ICs.[8]

In-house chamber design and fabrication

The in-house IC was designed based on the specifications of a Farmer-type IC. The body of the in-house IC was made up of three separate cylindrical pieces, namely: chamber sensitive volume cap, stem and stem continuation. The entire body of the in-house IC was composed of Perspex (PMMA) having a density of 1.18 g/cm^3.

The chamber's sensitive volume cap was designed and shaped into a cylindrical tube having dimensions of 40.00 mm in length, 15.90 mm external diameter, 7.80 mm internal diameter, and 4.05 mm wall thickness. The open end of the tube had a small recess (or groove) to receive portions of the stem. The cylindrical tube forming chamber sensitive volume cap was fashioned from a piece of the 20.00 cm length of solid Perspex (PMMA) rod. A schematic diagram of the chamber's sensitive volume cap is depicted in **Figure 1**.

A piece of paper with a width of 28.00 mm and a length similar to the internal circumference of the chamber's sensitive volume cap, was cut from the A4 paper sheet. One surface of the cut paper strip was entirely covered with Sterotape to make the paper strip firm and rigid. The 4B pencil was used to coat the other surface of the paper with graphite by rubbing the graphite tip of the pencil against the surface of the paper.

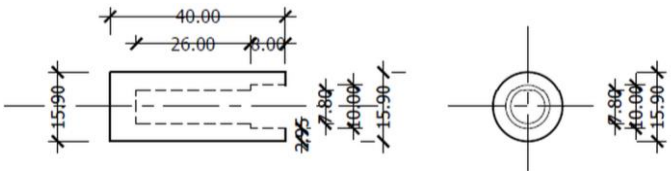

Figure 1. Schematic diagram of chamber's sensitive volume cap (all dimensions are in millimeters)

The coated surface of the paper was checked for electrical conductivity by measuring electrical resistance across the surface of the paper with the multimeter. The electrical conductivity measurement setup for the sample of the graphite-coated paper strip is shown in **Figure 2**.

The graphite-coated paper strip was used to cover the internal wall of the chamber's sensitive volume cap, such that the surface of the paper having the Sterotape was in contact with the internal wall of the chamber sensitive volume cap. This was done to make the chamber's sensitive volume cap electrical conductive as well as minimizing cost to be incurred in electroplating the chamber's sensitive volume cap with graphite.

The stem of the in-house IC was also fashioned from the remaining piece of the 15.90 mm diameter Perspex rod. The stem was fabricated to have the same constructional dimensions as the chamber's sensitive volume cap, but both ends were opened and one end shaped to form a tongue, which could fit perfectly into the recess (or groove) of the chamber's sensitive volume cap. The other end was designed to terminate into a recess (or groove). A schematic diagram of the stem is shown in **Figure 3**. The stem was made to hold the central and the polarizing electrodes of the IC.

The central electrode of the in-house IC was made of an aluminum rod having a length of 30.00 mm and a diameter of 1.78 mm. The aluminum rod formed part of strands of aluminum wires within a piece of scrapped aluminum twisted cable obtained from the country's main electricity provider. The central electrode was then connected to the central wire of the triaxial cable with a clamping mechanism designed at one end of the aluminum rod. A piece of cylindrical polystyrene plastic tube, open at both ends with a wall thickness of 1.00 mm, was used as an insulator to separate the central electrode from the polarizing electrode. Another similar plastic tube with a larger internal diameter was also used to separate the polarizing electrode from the ground electrode, as depicted in **Figure 4a**. **Figure 4b** shows the assembled in-house IC with the chamber sensitive volume cap removed exposing the central and ground electrodes.

All connections to the various electrodes with the triaxial cable were made within the stem. The triaxial cable and its connecting TNC male connector (as shown in **Figure 5**), which was used for the in-house IC, were salvaged from a discarded PTW extension triaxial cable. The said cable was used by the radiotherapy department for connecting its PTW electrometer at the console area to any IC within the treatment room during any radiation dosimetry involving an IC. The cable got severed and was discarded. A portion of the cable attached to the male connector was used. Before using the cable, continuity and electrical impedance tests were performed on the portion of the cable to be used to ascertain its suitability and reliability.

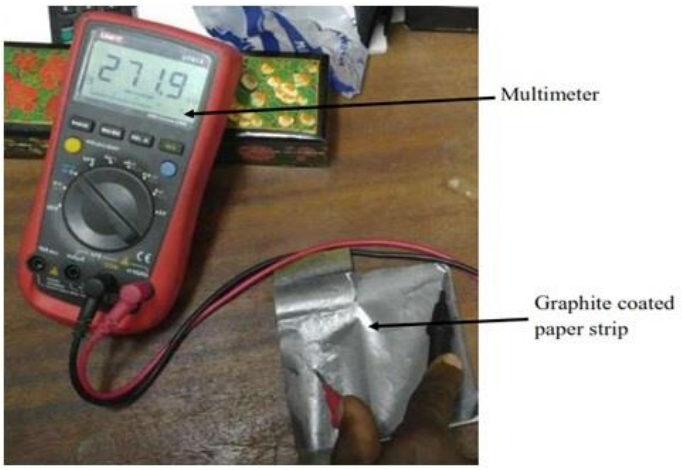

Figure 2. Testing of paper coated with graphite for conductivity

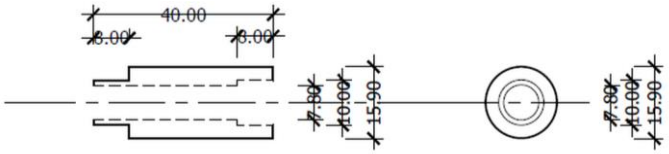

Figure 3. Schematic diagram of the stem of in-house IC (all dimensions are in millimeters)

Figure 4. Electrodes of the in-house IC: (A) Central electrode and insulator between polarizing electrode and ground electrode, and (B) Central and ground electrodes embedded in the stem of in-house IC

Figure 5. Male TNC connect (W Type)

The stem continuation was fabricated from a portion of the 20.00 cm long Perspex rod and was made to have similar physical dimensions as the stem of the in-house IC. The stem continuation had dimensions of 70.00 mm length, 15.90 mm external diameter, 5.00 mm internal diameter, and 5.45 mm wall thickness, as indicated in the schematic diagram in **Figure 6**. One end of the stem continuation was fashioned into a tongue such that it could fit perfectly into the recessed end of the stem. The central hole at the other end of the stem continuation having a length of 2.00 cm, was widened to 7.00 mm. A detached drainage tube of a urine bag was fixed into the 7.00 mm wide hole on the stem continuation and held in place with synthetic resin adhesive (Araldite glue). The connection between the stem continuation and the drainage tube of a urine bag was ensured to be waterproof by subjecting the assembled parts to a pressure test. The drainage tube of a urine bag used had a length and wall thickness of 87.00 cm and 0.36 mm, respectively. The external and internal diameters of the drainage tube were 6.48 mm and 5.76 mm, respectively. The triaxial cable was made to pass through the stem continuation and the drainage tube assembly before making its way to the stem. These were done to make the in-house ionization waterproof, such that it can be immersed directly into the water.

The various interlocking body parts of the in-house IC were put together and glued in place with Chloroform (Trichloromethane), a solution that dissolves Perspex. How the various body parts of in-house IC were joined together is depicted in **Figure 7**. After gluing the various parts together, the whole assembly was subjected to a pressure test to ensure that the joint portions were air-tight. The sensitive volume of the in-house IC was vented to the environment via the attached drainage tube of a urine bag which covered portions of the triaxial cable attached to the IC. The completed in-house IC is shown in **Figure 8**.

Pre-evaluation of the fabricated in-house IC

The following dosimetric characteristics of the constructed in-house IC were studied to assess the performance of the IC as well as to ascertain if the fabricated IC could satisfy the international standards as stipulated by IEC 60731:2011.[8] The dosimetric characteristics studied were: effects of bias voltage on the detector response, polarity effects, angular dependence in terms of beam incidence, dose linearity, dose rate dependence, beam quality dependence, stem effect, short term, medium term, and long term stabilities, and pre- and post- irradiation leakage currents. A calibration coefficient was also established for the fabricated IC.

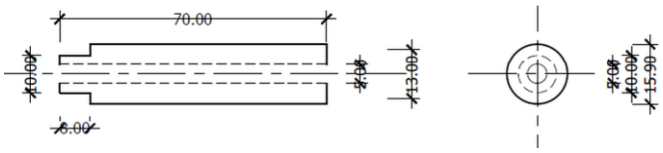

Figure 6. Schematic diagram of stem continuation of in-house IC (all dimensions are in millimeters)

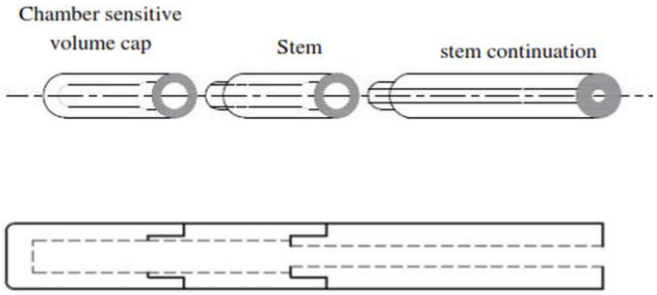

Figure 7. Interlocking of chamber sensitive volume cap, stem, and stem continuation

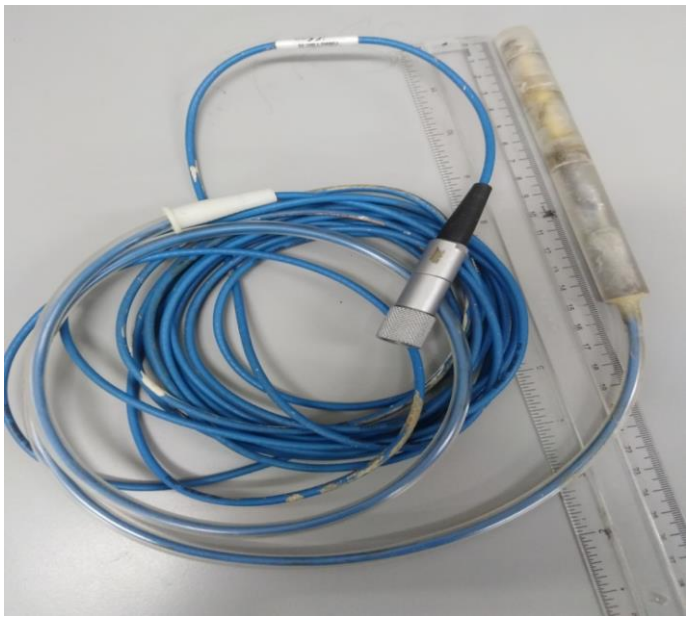

Figure 8. Completed in-house IC

Measurements to study the effects of chamber bias voltage on chamber response were carried out with the Equinox 100 telecobalt machine (Best Theratronics, Canada). During the measurements, the fabricated IC was connected to the PTW UNIDOS electrometer (SN: T10002-020204; PTW Freiburg, Germany), which was set to measure charges in an integral mode for 60 s intervals. Electrometer readings were obtained for chamber bias voltages ranging from 100 to 400 V (increment of 50 V) with both positive and negative polarities. The measurements were done at a depth of 5 cm on the beam central axis in the PTW MP1 manual motorized water tank phantom (SN: T41025-000067; PTW Freiburg, Germany) using an open field of 10 cm × 10 cm, employing source-to-surface distance (SSD) irradiation technique (with SSD = 100 cm). A chamber

holder was designed and constructed from Perspex to enable the fabricated IC to be held within the water phantom. The water phantom with the IC held within it during the measurements is shown in **Figure 9**. The measured results obtained were also used to determine the polarity effect, ion recombination correction factor or saturation factor, and ion collection efficiency associated with the IC. These properties of the IC were determined based on the International Atomic Energy Agency (IAEA) technical report series 398 protocol.[5] In all the measurements, it was ensured that there was at least 10 cm of water below the IC to provide the needed backscatter radiation.

The setup used to study the effects of bias voltage on detector response was also used to study pre-irradiation and post-irradiation leakage current characteristics of the constructed in-house IC. During the pre-irradiation leakage current test, the chamber was not exposed to any radiation after connecting to the electrometer. After switching on the electrometer, the leakage current was monitored for 100 s intervals with the electrometer set to measure radiation in continuous mode using a bias voltage of +400 V. For the post-irradiation leakage current test, the chamber was irradiated for 10 min with the electrometer set in radiation trigger mode (or continuous mode) before the irradiation. The electrometer reading after the irradiation was noted and recorded, and the electrometer reading was monitored for another 5 s. The bias voltage of the electrometer was maintained at +400 V. The electrometer reading at the end of the 5 s was also recorded. The change in electrometer reading before and after the 5 s was determined. These measurements were repeated five (5) consecutive times.

The dose linearity test was conducted using the experimental setup used for the post-irradiation leakage current evaluation of the in-house IC. The IC was irradiated with known doses ranging from 0.4 to 5.2 Gy (increments of 0.4 Gy) with beams from both the telecobalt machine and the Elekta Synergy® platform medical linear accelerator (Elekta Instrument AB Stockholm, Sweden). The doses were converted to their corresponding treatment times and monitor units for the telecobalt machine and the linear accelerator (linac), respectively based on the IAEA TRS 398 protocol[5] with traceability to the PTW-Freiburg calibration laboratory, Germany. The electrometer readings obtained were corrected for variations in air density. For the irradiations with the linac, the depth of measurement was set at 10 cm, and a beam energy of 15 MV was used. Also, prior to the measurements with a treatment machine, the IC was pre-irradiated for 15 min to remove stray charges within the chamber. The corrected electrometer readings were plotted against their corresponding doses for each teletherapy machine. Since further assessments of the in-house IC would be made with 15 MV beams from the linear accelerator, the beam quality factor, $k_q^{in-house}$, of the 15 MV beam for the in-house IC was determined.

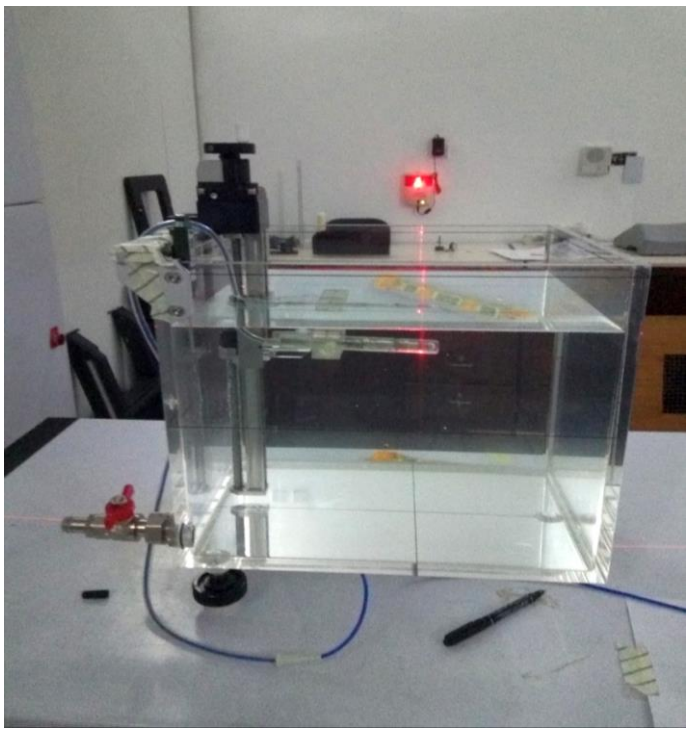

Figure 9. Water phantom with fabricated IC held within during measurements

The substitution interpolation (SI) approach was adopted for the determination of the beam quality factor. The approach entailed: beam output calibration measurements of the 15 MV beam from the linac with the in-house IC employing the IAEA-TRS 398 protocol[5] and then repeating the measurements with the 0.6 cc Farmer type IC (TN 30013-009262; PTW-Freiburg, Germany). The beam quality factor of the PTW 0.6 cm^3 Farmer type IC for the 15 MV beam, k_q^{PTW}, was established through the measurement of the beam quality specifier (BQS), $TPR_{20,10}$ with the 15 MV beam.[5] Also, during these measurements, both ICs were connected to the PTW UNIDOS electrometer. The beam quality factor of the in-house IC for the 15 MV beam was calculated as:

$$k_q^{in-house} = \frac{M_{cor.}^{PTW} \times N_{D,W}^{PTW} \times k_q^{PTW}}{M_{cor.}^{in-House} \times N_{D,W}^{in-House}} \quad \text{Eq. 1}$$

where: $M_{cor.}^{in-House}$ and $M_{cor.}^{PTW}$ are the corrected electrometer readings for the beam output measurements with the in-house and the PTW ICs, respectively, and $N_{D,W}^{in-House}$ and $N_{D,W}^{PTW}$ are the cobalt- 60 calibration coefficients of the in-house and the PTW ICs, respectively.

The final step of the SI approach involved measurements to establish beam quality factor characteristics of the in-house IC. BQS, $TPR_{20,10}$ was also measured with the in-house IC for the 15 MV beam from the linac. The obtained $TPR_{20,10}$ and $k_q^{in-house}$ for the in-house IC were used to find an IC within the k_q table of the IAEA-TRS 398[5] whose beam quality factor was comparable to $k_q^{in-house}$ based on the obtained BQS value obtained for the in-house IC.

Short term and medium term stability assessments of the in-house IC were conducted with the telecobalt machine using the setup used for the dose linearity test, but the electrometer was set to measure radiation at 60 s intervals. For the short term stability assessment, twenty-five (25) successive electrometer readings were taken with beam-on. Prior to these measurements, the setup was allowed 8 hours to acclimatize to the treatment room temperature. The mean of the 25 electrometer readings was determined, and each electrometer reading was normalized to the obtained mean value. A graph of electrometer reading related to the mean value as a function of time elapsed after switching on the electrometer was plotted. For the medium-term stability check, using the same setup as that used for short-term stability assessment, beam outputs of the telecobalt machine were measured with the in-house IC every weekend for a period of two months based on the IAEA TRS 398 protocol.[5] Decay corrections were applied to the measured dose rates (weekly beam outputs) to check if they were comparable to the initial dose rate measured for the telecobalt machine. Before these measurements, the calibration coefficient of the in-house IC was determined by a cross-calibration procedure using the substitution method, according to the methodology proposed in the IAEA-TRS 374.[6] Using a setup similar to that used for the stability assessments, the constructed in-house IC was cross-calibrated against the PTW 0.6 cm^3 cylindrical Farmer type IC with a calibration coefficient traceable to the national standard of the Germany National Laboratory, PTB, Germany. Measurements to determine the calibration coefficient of the in-house IC were performed with the telecobalt machine.

Measurements to assess dose rate dependency of the constructed IC were carried out with the linear accelerator using a setup similar to that used for the post-irradiation leakage current evaluation. Electrometer readings were obtained on the beam central axis at a depth of 10 cm when the constructed IC within the water phantom was exposed to a dose of 77 cGy (100 MU) using varying dose rates ranging from 100 to 600 MU/min (increment of 100 MU/min). Photon beam energy of 15 MV was used for the irradiations. For the energy dependency check, measurements were done with both cobalt-60 and 15 MV photon beams while maintaining the same setup. The constructed IC was positioned at depths of 5 and 10 cm within the water phantom for irradiations with the telecobalt machine and the linear accelerator, respectively. For each of the treatment machines, a dose of 2 Gy was delivered to the point of measurement. Electrometer readings after the irradiations were recorded. The obtained electrometer readings for the dependencies assessment were corrected for variations in air density.

Stem effect assessments of the in-house IC were performed with the telecobalt machine employing two independent methods. For the first method, collimator scatter factors (S_c)[9] were measured with the in-house house, the PTW 0.6 cm^3 cylindrical and the PTW 0.125 cm^3 Semiflex ICs for square field sizes having one side of square field size of 4, 6, 8, 10, 15, 20, 30, and 40 cm, using radiation source to detector distance of 100 cm. Collimator scatter factors are defined as the ratios of the dose measured with a detector at a reference point in air along the beam central axis for a given field to the dose at the same point for a field of 10 cm × 10 cm. Using the same axes, a graph of S_c against one side of a square field size was plotted for the detectors. In the second approach, doses were measured with the in-house IC on the beam central axis at a depth of 5 cm in the Blue phantom[2] motorized water tank (IBA Dosimetry, Germany) for different elongated rectangular field sizes with beams coming from the telecobalt machine. SSD irradiation technique (SSD = 100 cm) was used for these measurements. The field sizes used were: 6 × 10, 6 × 20, 6 × 30, 6 × 35, 10 × 20, 10 × 30 and 10 × 35 cm^2. For each field size, the dose measurement was also repeated with the x- and y-jaws collimator settings interchanged. The measured doses were corrected for variations in air density. The stem effect associated with the constructed IC, S_{eff}, expressed as a percentage of the measured dose for a particular field size setting was obtained from the expression[8]:

$$S_{eff} = \frac{M_1 - M_2}{M_1} \times 100\% \quad \text{Eq. 2}$$

where M_1 and M_2 are corrected electrometer readings for measurements with stipulated elongated rectangular field size and that with the x- and y-jaws collimator settings of the field size interchanged.

The angular dependence of the in-house IC was assessed with the telecobalt machine. The measurements were performed in air using a source to detector distance (SDD) of 100 cm. The chamber's long axis was positioned to coincide with the isocenter of the telecobalt machine. An open field of 10 × 10 cm^2 was used for the various measurements using gantry angles ranging from 0° to 345° (increments of 15°). The experimental setup used for the assessment of the angular dependence of the in-house IC is depicted in **Figure 10**. The gantry of the telecobalt machine was rotated around the detector in a clockwise direction with the detector mounted on a carbon fibre rod, such that the geometrical center of the IC was aligned with the isocenter of the treatment machine. For each gantry angle, the response of the in-house IC was recorded with the UNIDOS electrometer connected to the IC, which was set to measure charges at 60 s intervals. The chamber responses were corrected for variations in air density, and corrected responses normalized to that of the gantry angle of 0°. A graph of relative response as a function of gantry angle was plotted.

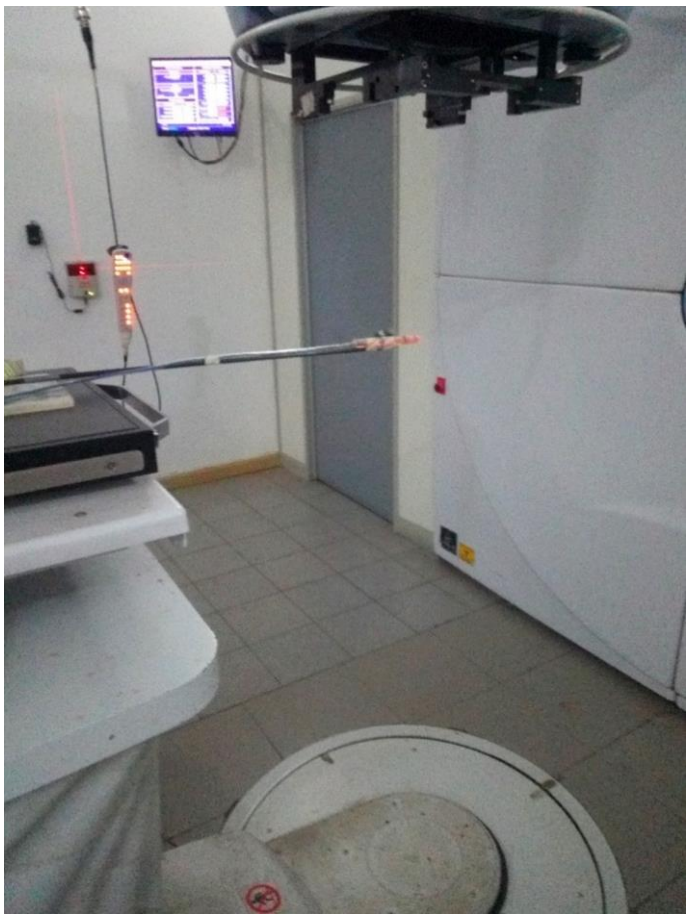

Figure 10. Setup to check angular dependence of in-house IC

Long term stability of the constructed IC was ascertained with the cobalt-60 teletherapy machine after two years of evaluating the other performance characteristics of the IC. The beam output of the telecobalt machine was measured with the constructed IC based on the IAEA-TRS 398 protocol using a similar setup which was used in evaluating the medium-term stability of the IC. The previously determined calibration coefficient of the IC was used to obtain the dose rate, DR_{meas}, at the depth of 5 cm along the beam central axis of the field size of 10 cm × 10 cm. The measurement was repeated with the PTW-Freiburg IC, which had just returned from a secondary standard dosimetry laboratory after recalibration. In obtaining the dose rate, DR_{ref}, with the commercial IC, the new calibration coefficient of the IC was used. The percentage variation in the beam output among the ICs, $DRV_{5\,cm}$, was calculated as:

$$DRV_{5cm} = \frac{DR_{meas} - DR_{ref}}{DR_{ref}} \times 100\% \qquad \text{Eq. 3}$$

Before these measurements, the constructed IC was once again subjected to short-time stability check by repeating the previous test. This was done to ascertain the reproducibility of the response of the detector.

Results

The effects of bias voltage on the response of the in-house IC are depicted graphically in **Figure 11**. The figure shows a graph of chamber response as a function of bias voltage for positive and negative bias voltages plotted using the same axes. Within the legend display on the graph are correlation equations and regressions (R^2) for the lines of best fit for the chamber responses with positive and negative bias voltages, respectively, which are enclosed in brackets. To distinguish between the correlation equations, the lines of best fit are identified by different line styles. Just after a correlation equation for a particular line of best fit is its regression (R^2), separated from the correlation equation by a semicolon.

Pre-irradiation leakage current characteristic of the in-house IC is depicted in **Figure 12**, which shows the variation of electrometer reading with elapsed time when the in-house IC was connected to the electrometer and the electrometer switched on without irradiating the IC. Above the curve in **Figure 12** are displayed the correlation equation and its corresponding regression, R^2 of the line of best fit.

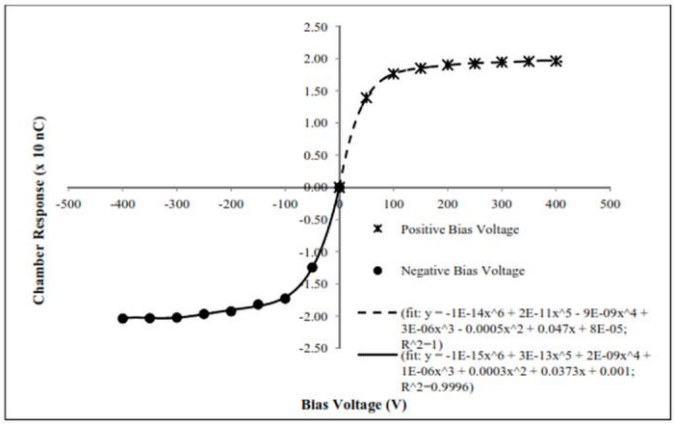

Figure 11. In-house chamber response as a function of bias voltage

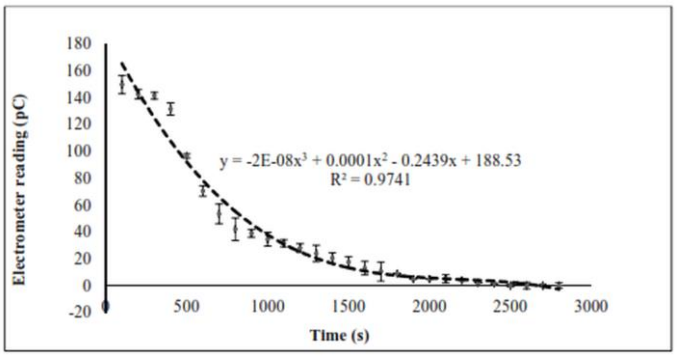

Figure 12. Pre-irradiation leakage current associated with in-house IC

Table 1. Parameters to study post-irradiation leakage current characteristic of in-house IC

Measurement Date	Electrometer reading for 10 min of irradiation, M_i (× 10^2 nC)			Electrometer reading 5 seconds post-irradiation, M_f (× 10^2 nC)			Percentage Diff. $\left(\frac{M_f - M_i}{M_i} \times 100\%\right)$		
	1	2	3	1	2	3	1	2	3
25-02-2018	1.958	1.954	1.958	1.959	1.955	1.959	0.051	0.051	0.051
31-03-2018	1.839	1.840	1.838	1.840	1.841	1.839	0.054	0.054	0.054

Table 2. Ion collection properties of in-house IC

Bias Voltage, V (V)	Raw mean electrometer reading, M_{raw} (× 10 nC)	Electrometer reading corrected for polarity, $M = M_{raw} \times K_{pol}$ (× 10 nC)	Air density correction factor, $K_{t,p}$	Polarity effect, K_{pol}	Ion recombination correction factor, K_s	Ion collection efficiency, $f_{ion} = 1/K_s$
400	1.8890	1.9030	1.0245	1.0074	1.0072	0.9928
350	1.8850	1.8935	1.0245	1.0045	1.0086	0.9914
300	1.8810	1.8812	1.0245	1.0001	1.0104	0.9897
250	1.8650	1.8441	1.0245	0.9888	1.0176	0.9827
200	1.8490	1.8113	1.0247	0.9796	1.0251	0.9755
150	1.8240	1.7417	1.0248	0.9549	1.0365	0.9648
100	1.7220	1.5873	1.0250	0.9218	1.0835	0.9229
-100	-1.7590	-1.6540	1.0226	0.9403	1.0217	0.9788
-150	-1.7830	-1.7368	1.0236	0.9741	1.0237	0.9769
-200	-1.8510	-1.8498	1.0235	0.9993	1.0177	0.9826
-250	-1.8700	-1.8863	1.0233	1.0087	1.0194	0.9810
-300	-1.8970	-1.9354	1.0231	1.0203	1.0219	0.9786
-350	-1.9090	-1.9562	1.0230	1.0247	1.0157	0.9845
-400	-1.9170	-1.9701	1.0228	1.0277	1.0119	0.9883

In **Table 1** electrometer readings are listed for 10 min of irradiating the in-house IC with cobalt-60 beams, and that obtained by observing the electrometer for a period of 5 seconds at the end of each of the 10 min irradiation for two different days. The change in electrometer reading between the 10 min irradiation period and the stipulated post-irradiation period is expressed as a percentage of the obtained electrometer reading for the 10 min irradiation for each of the various consecutive readings per day. The percentage differences used to study post-irradiation leakage current characteristics of the in-house IC are also enumerated in **Table 1**.

Table 2 lists measured parameters used to express ion collection characteristics of the constructed in-house IC. Mean values of uncorrected electrometer readings obtained at 60 s intervals with the in-house IC at various bias voltages for the cobalt-60 beam, and their corresponding determined: air density, polarity effect, and ion recombination correction factors, as well as ion collection efficiencies of the in-house IC, are listed in **Table 2**. The content of **Table 2** also includes values of mean electrometer readings corrected for the polarity effect. The corrected electrometer readings together with their corresponding bias voltage were used to produce a Jaffé diagram[10,11] for the in-house IC as shown in **Figure 13.**

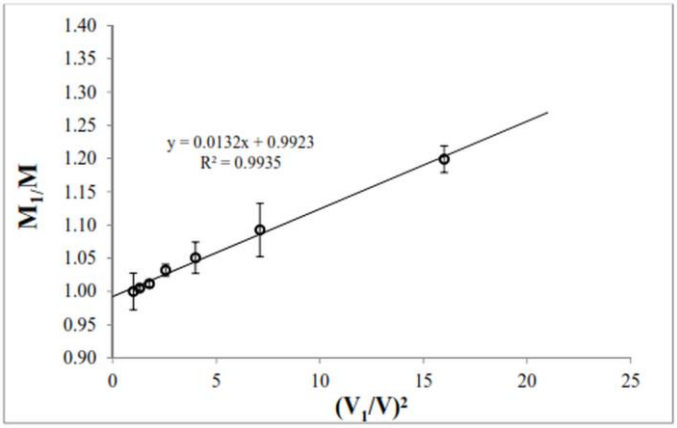

Figure 13. Jaffé diagram for in-house IC operated at $V_1 = 400\ V$

Figure 13 is used to represent the inverse electrometer reading, $1/M$ of the in-house IC as a function of the inverse square of the applied bias voltage, $1/V^2$. **Figure 13** shows a Jaffé diagram for a continuous radiation with axes normalized to usual voltage, V_1 used to calibrate the IC and its corresponding electrometer reading, M_1. Since the chosen operating bias voltage, $V_1 =$ 400 V, is positive, positive bias voltages, V, were used to obtain the bias voltage ratios for the Jaffé plot.

The dose linearity of the in-house IC for 15 MV and cobalt-60 beams is depicted in **Figure 14**. **Figure 14** shows graphs of in-house IC response against dose for beam energies of 15 MV and cobalt-60, respectively. On each of the graphs are displayed correlation equation and their corresponding regression, R^2 of the line of best fit.

The short-term and medium-term stabilities of the in-house IC are demonstrated graphically in **Figure 15a** and **Figure 15b**, respectively. **Figure 15a** shows a dot plot of chamber response (electrometer reading in nC) normalized to the mean of chamber responses obtained for twenty-five (25) consecutive readings against the reading number (measurement). **Figure 15b** also shows a dot plot of the percentage difference between a measured dose for a week (after applying the necessary decay correction) and that measured for the first week against the week number. The dashed lines on the plots in **Figure 15** represent the limits according to IEC 60731.[8]

Results of the angular dependence test of the in-house IC are presented graphically in **Figure 16**, which depicts dot plot of chamber response normalized to that of 0° degree gantry angle against gantry angle. The black and red dashed lines represent the limits according to IEC 60731[8] and IAEA-TRS 398[5], respectively.

Figure 17 shows a graph of the collimator scatter factor as a function of one side of a square field side measured for the telecobalt machine with both the in-house IC and the two commercial ICs. The collimator scatter factors of the ICs are plotted using the same axes. Attached to the legend display on the graph and enclosed in brackets are correlation equations and their corresponding regressions, R^2 of the lines of best fit. The lines of best fit are indicated by different line styles and colours.

Parameters to obtain for the various elongated field sizes to study the stem effect of the in-house IC are listed in **Table 3**. Also listed in **Table 3** are the calculated stem effects for the various field sizes obtained using **Equation 2**.

Table 3. Parameters to evaluate stem effect of in-house IC

Field size (cm^2)		Electrometer Reading (× 10 nC)		Diff. in Reading ($M_1 - M_2$)	Stem effect (%)
1	2	M_1	M_2		
6 × 10	10 × 6	1.885	1.882	0.03	0.18
6 × 20	20 × 6	1.959	1.943	0.14	0.73
6 × 30	30 × 6	1.997	1.970	0.29	1.40
6 × 35	35 × 6	1.998	1.977	0.20	1.02
10 × 20	20 × 10	2.046	2.047	-0.01	-0.06
10 × 30	30 × 10	2.086	2.087	-0.01	-0.06
10 × 35	35 × 10	2.093	2.098	-0.05	-0.24

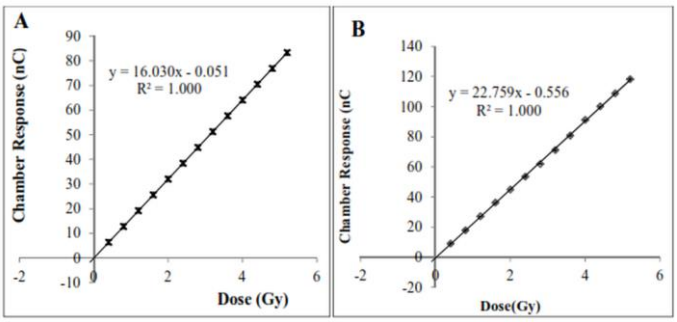

Figure 14. Graphs of chamber response against dose for beam energies of: A. 15 MV and B. cobalt-60, respectively

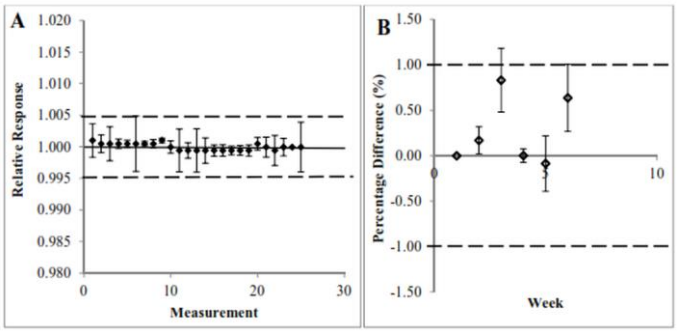

Figure 15. Graphical representation of response constancy and reproducibility of in-house IC: (A) short-term stability, and (B) medium-term stability

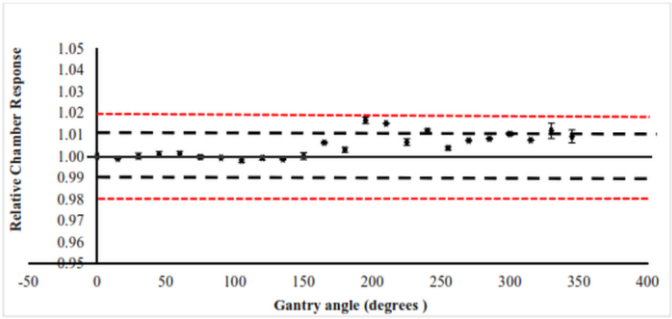

Figure 16. Angular dependence test of the in-house IC

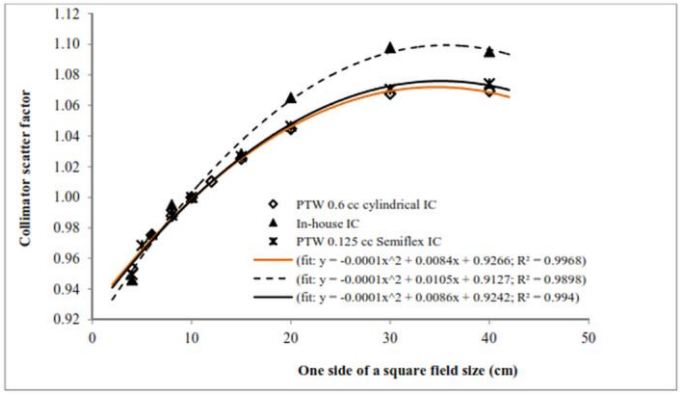

Figure 17. Collimator scatter factors measured with commercial ICs and in-house IC

In **Table 4** are listed mean electrometer readings obtained with different dose rates for the irradiations of the in-house IC in the water phantom with beams from the linac. The electrometer readings are normalized to that of the dose rate of 100 MU/min. The normalized electrometer readings are also presented in **Table 4**.

For the long-term stability, the beam outputs measured with the commercial and the constructed IC were 49.14 cGy/min and 50.42 cGy/min, respectively. The percentage variation in the dose rates calculated with **Equation 3** is 2.6%. In **Figure 18** is shown the short-term stability of the constructed IC after two years of initial evaluation, and before the measurement of the telecobalt machine beam output with the constructed IC.

Table 4. Dose rate dependence of in-house IC

Dose Rate (MU/min)	Mean electrometer reading (nC)	Normalized mean electrometer reading
100	15.395 ± 0.015	1.0000
200	15.420 ± 0.022	1.0016
300	15.405 ± 0.019	1.0006
400	15.415 ± 0.021	1.0013
500	15.450 ± 0.025	1.0036
600	15.390 ± 0.010	0.9997

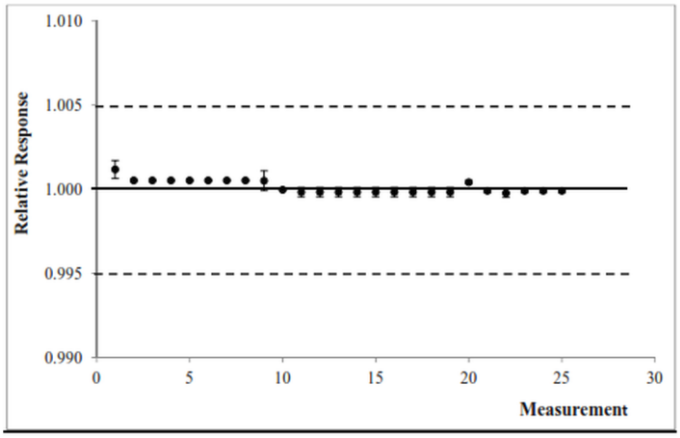

Figure 18. Short term stability of constructed IC after two years of previous measurement

Discussions

Composing the entire body of the in-house IC with Perspex makes the in-house IC more tissue-equivalent when immersed in water during measurements. This property of the in-house IC, coupled with the diameter of its central electrode (greater than 1 mm), make the constructed IC more sensitive to low-energy scattered radiation. This is envisaged in **Figure 17**, where the variation of S_c with field size measured with the in-house IC is being compared to those of the commercial ICs. For larger field sizes, where low scattered radiations are more pronounced, the response of the in-house IC is higher than those of the commercial ICs, and the opposite of these is conspicuous for the small field sizes (below 10 cm × 10 cm). Also, the over-response of the in-house IC can be attributed to the stem effect (leakage current generated when the chamber stem is included in the radiation field size), which can be divided into stem leakage and stem scatter.[12] These interactions contribute to the apparent measured exposure.[12] Since the chamber irradiations were done in the air, the chamber response is likely to be affected by the photons scattered from the chamber stem. Photon scattered from the chamber stem, which is a function of the chamber stem included in the radiation field size, is likely to be more pronounced for the in-house IC than the commercial ICs owing to the nature and composition of the chamber stem of the in-house IC. The differences in the measured S_c for the commercial ICs for field sizes greater than 10 cm × 10 cm are as a result of volume averaging effect.[13]. To give the in-house IC its robustness, its Perspex wall (constituting chamber stem and sensitive volume) was made quite thick, which is enough to provide the needed build-up for cobalt 60 beam energy for in-air measurements. The wall thickness of the in-house IC can be considered as a contributing factor why for highly elongated radiation field sizes, the detector cannot meet the IEC 60731; 2011 recommended limit for stem effect of ±1.00%.[8] The stem effect can also originate from the chamber cable. In **Table 3**, for field sizes of 6 cm × 30 cm and 6 cm × 35 cm, the measured stem effects are 1.40% and 1.02%, respectively, which are slightly higher than the recommended value.

These effects can be reduced or made quite negligible with the introduction of an appropriate guard electrode (ring) in the design and construction of the in-house IC, such that charges that are generated outside the sensitive volume of the chamber are not collected to influence the chamber reading. Also, the guard electrode coupled with the enhancement of electrical insulation between the various electrodes of the constructed IC can be used to reduce leakage current associated with the constructed IC. The guard electrode of an IC is used to remove stray or unwanted charges to the earth (ground). From **Figure 12**, it shows that the constructed IC needs about 45 min to stabilize when connected to an electrometer, hence one needs to wait for that period to elapse before the commencement of measurements with the chamber. This is attributed to stray charges within the sensitive volume of the chamber. Regarding the stem effect and leakage current associated with the constructed IC, an upgraded version of the IC is being constructed such these effects are made very marginal. From the results of the angular dependence test depicted graphically in **Figure 16**, it shows that there is a slight variation in wall thickness across the circumference of the chamber for the constructed IC. The results show that the anomaly in wall thickness is prone to one-half of the chamber. This may also be attributed to setup uncertainties. Nevertheless, the anomaly may be considered marginal as all the test points are within the IAEA limit (83.33% are within the IEC limit).

Measurement of the polarity effect associated with a dosimetry system is a very simple quality assurance check to determine the suitability of using the dosimetry system for

reference dosimetry.[14] ICs preferred for reference dosimetry are recommended to have polarity effects associated with the ionization chamber/electrometer ranging from 0.996 to 1.004 (or less than 0.4% correction is required).[14] The constructed IC shows voltage-dependent polarity effects, as presented in **Table 2**. The polarity effect increases with increasing chamber bias voltage. The constructed IC is, therefore, able to satisfy the recommended polarity effect for reference dosimetry when operated with bias voltages ranging from 300 to 350 V. This is in tandem with the AAPM-TG 51 addendum recommended bias voltage of 300 V for ICs preferred for reference dosimetry.[14] Howbeit, from **Table 2**, ion recombination correction factors for this bias voltage range are higher than that of 400 V, hence the choice of the 400 V as the operating voltage of the constructed IC. Though in some cases the higher bias voltage may result in charge multiplication within the sensitive volume of an ionization chamber, this phenomenon can be evaluated by ion collection efficiency within the 'ion chamber' and the magnitude of the required recombination correction which should be less than 2%.[14,15,16] The aforementioned characteristics for the in-house IC at the bias voltage of 400 V are within tolerance, hence charge multiplication in the sensitive volume of the IC is expected to be negligible. The potential sources of the polarity effect may be due to: secondary electron emission producing negative current independent of the polarity of the electrode, low energy electron ejection from the chamber wall, which is not compensated by collecting electrode, uneven distribution of the space charge, virtual variation of active volume due to space charge distortion, stopping of the fast electrons in the collecting electrode not balanced by the ejection of the recoil electrons, collection of current outside the chamber sensitive volume due to leakage in the solid insulator, and design deficiencies in guard ring (or electrode). Improvement in guard electrode design and enhancement of insulation between the various electrodes of the constructed IC can be used to reduce the polarity effect correction factor of 1.007 obtained at the operating bias voltage of 400 V to fall within the recommended range stipulated by the AAPM-TG 51 addendum.[14]

The Jaffé diagram in **Figure 13** shows that the regression line to the linear part intersects the M_1/M axis at 0.9923 resulting in an ion recombination correction factor, $k_s = {}^{1}/_{0.9923}$=1.0078. This is slightly higher than that obtained with the two bias voltages technique presented in **Table 2** for the same usual (or operating) bias voltage of 400 V. The linear part of the Jaffé diagram also depicts a useful range for the chamber bias voltage within which the constructed IC should be operated. The Jaffé plot approach of determining the ion recombination correction factor is more accurate than the two voltages technique.[17,18]

Notwithstanding the performance of the constructed IC, there is the need to subject the IC to a long-term stability test, where the output constancy of the IC would be assessed over two years. The choice of beams from the telecobalt machine to evaluate the long-term stability of the constructed IC after two years was due to the stableness of beam characteristics of a telecobalt machine.[19] For this evaluation, the response of the in-house IC was compared to that of a calibrated commercial IC to eliminate ambiguities with the application of a decay correction. Although the reproducibility of successive readings obtained at regular intervals with the in-house compared very well with that of two previous years, the output comparison shows that the performance of the in-house IC had drifted by 2.6%, which is more than the 2.0% recommended by the IEC 60731 for long term stability. Concerning this, there is, therefore, the need to recalibrate the in-house IC annually. And from **Figure 18**, it can be affirmed that the short-term stability of the constructed IC has not changed significantly after two years, making it possible for the IC to be used for absolute dosimetry.

The results obtained for the pre-evaluation tests conducted on the in-house IC put the chamber in a better position to be used for therapy megavoltage photon beam output calibration. However, there is a need to improve certain features of the in-house IC to make it compete with commercially available Farmer-type ICs. This will go a long way in helping radiation oncology facilities in developing countries meet their reference dosimetry requirements at a reduced cost.

Conclusion

A large volume waterproof vented IC to be used for reference dosimetry of therapy beams has been constructed from locally available materials to minimize the cost of construction. Although pre-evaluation tests based on international standards performed on the constructed IC show that the IC is suitable for reference dosimetry of therapy beams, there is the need to enhance insulation between the various electrodes of the IC, as well as incorporate appropriate guard electrode into the design of the IC. These requirements are needed to reduce leakage current associated with the IC.

Acknowledgement

This publication is a refined extract of the thesis submitted to the University of Ghana, Legon, Ghana, by Mr. Clement Chaphuka in partial fulfilment of the award of a Master of Philosophy degree in Medical Physics having the corresponding author as the principal supervisor and the other author as a member of the supervisory team.

References

1. International Commission on Radiation Units and Measurements (ICRU). ICRU Report 24. Determination of absorbed dose in a patient irradiated by beams of x or gamma rays in radiotherapy procedures. International Commission on Radiation Units and Measurements. Bethesda, Maryland. 1976.
2. van der Merwe D, Van Dyk, J, Brendan H, et al. Accuracy requirements and uncertainties in radiotherapy: a report of the International Atomic Energy Agency. Acta Oncologica. 2017;56(1):1-6. 10.1080/0284186X.2016.1246801
3. Podgorsak EB. Radiation Oncology Physics: A handbook for teachers and students. International Atomic Energy Agency (IAEA), Vienna. 2005.
4. Almond PR, Biggs PJ, Coursey BM, et al. AAPM's TG-51 protocol for clinical reference dosimetry of high-energy photon and electron beams. Med Phys. 1999;26(9):1847-1870. https://doi.org/10.1118/1.598691
5. International Atomic Energy Agency (IAEA).Technical report series 398. Absorbed dose determination in external beam radiotherapy. IAEA, Vienna. 2000.
6. International Atomic Energy Agency (IAEA). Technical report series 374. Calibration of Dosimeters Used in Radiotherapy. IAEA, Vienna. 1994.
7. Gibbons JP, Antolak JA, Followill DS, et al. Monitor unit calculations for external photon and electron beams: Report of the AAPM Therapy Physics Committee Task Group No. 71. Med Phys. 2014;41(3):031501. https://doi.org/10.1118/1.4864244
8. International Electrotechnical Commission. Medical Electrical Equipment- Dosimeters with Ionization Chambers as Used in Radiotherapy, IEC 60731, IEC, Geneva. 2011.
9. Khan FM. The Physics of Radiation Therapy (4th ed.). Lippincott Williams and Wilkins. 2010.
10. Besheli MG, Simiantonakis I, Zink K, Budach W. Determination of the ion recombination correction factor for intraoperative electron beams. Zeitschrift für Medizinische Physik. 2015;26(1): 35-44. https://doi.org/10.1016/j.zemedi.2015.06.011
11. Physikalisch-Technische Werkstätten (PTW). Ionization radiation detectors: Including codes of practice. PTW-Freiburg, Germany. 2009.
12. Kweon DC, Lee JS, Goo EH, et al. An Overall Stem Effect, including Stem Leakage and Stem Scatter, for a TM30013 Farmer-type Chamber. Journal of the Korean Physical Society. 2011;58(6):1688-1696. https://doi.org/10.3938/jkps.58.1688
13. Low DA, Parikh P, Dempsey JF, Wahab S, Huq S. Ionization chamber volume averaging effects in dynamic intensity modulated radiation therapy beams. Med Phys. 2003;30(7):1706-1711. https://doi.org/10.1118/1.1582558
14. McEwen MR, DeWerd L, Ibbott G, et al. Addendum to the AAPM's TG-51 protocol for clinical reference dosimetry of high-energy photon beams. Med Phys. 2014;41(4):041501. https://doi.org/10.1118/1.4866223
15. Wang Y, Easterling SB, Ting JY. Ion recombination corrections of ionization chambers in flattening filter-free photon radiation. J Appl Clin Med Phys. 2012;13(5):262-268. https://doi.org/10.1120/jacmp.v13i5.3758
16. Hyun MA, Miller JR, Micka JA, DeWerd LA. Ion recombination and polarity corrections for small-volume ionization chambers in high-dose-rate, flattening-filter-free pulsed photon beams. Medical Physics. 2017;44(2):618-627. https://doi.org/10.1002/mp.12053
17. Kry SF, Popple R, Molineu A, Followill DS. Ion recombination correction factors (P(ion)) for Varian TrueBeam high-dose-rate therapy beams. J Appl Clin Med Phys. 2012;13(6):318-325. https://doi.org/10.1120/jacmp.v13i6.3803
18. El-Moataz AB, Abouelenein HS, Ammar H, Khalil MM, El-Nagdy MS. Evaluation of the Characteristics of Ionization Chambers Used for Commissioning in High Dose Rate Linacs. Insights Med Phys. 2019;4(1):1.
19. Walter AE, Hansen JB, DeWerd LA. Evaluation of ionization chamber stability checks using various sources. Phys Med. 2020;80:327-334. https://doi.org/10.1016/j.ejmp.2020.11.010